Mechanical Properties of Frozen Glacial Tills due to Short Periods of Thawing

Yanju Fu [1,3], Yao Jiang [1,2,3]*, Jiao Wang [1,2]*, Ziming Liu [1,3] and Xingsheng Lu [1,3]

[1]Key Laboratory of Mountain Hazards and Earth Surface Process, Institute of Mountain Hazards and Environment, Chinese Academy of Sciences (CAS), Chengdu, China, [2]China-Pakistan Joint Research Center on Earth Sciences (CAS-HEC), Islamabad, Pakistan, [3]University of Chinese Academy of Sciences, Beijing, China

Due to the warming climate, glacier retreat has left massive glacial tills in steep gullies; ice in the soil is prone to change phase resulting in the decrease of the ice strength and bonding of soil particles; collapse of thawing tills can lead to debris flows with disastrous consequences for geotechnical infrastructures. To improve our understanding of the mechanics of thawing glacial tills, we conducted unconsolidated–undrained direct shear tests on glacial tills from Tianmo gully on the southeastern Tibetan Plateau. Control specimens were not subjected to freeze–thaw action. A total of 648 specimens with three different dry densities, three initial water contents, and 18 thawing times were tested. Peak shear strength, peak stress to displacement ratio (0.857), and cohesion were the highest in frozen specimens. After a thawing time of 0.25 h, there was a marked decline in shear strength; maximum friction was 2.58, which was far below the value of cohesive strength. For thawing times of 0.25–4 h, peak strength varied little with thawing time, but cohesion decreased and internal friction angle increased with increasing thawing time. Our results indicate that thawing of the solid ice in the till during the initial phase of till thawing is the key control of peak till strength; the effect of ice on cohesion is greater during the initial phase of thawing and in loose tills. Moreover, frequent sediment recharge of gullies may be explained by the decrease of cohesion with increasing thawing time caused by short-term destruction of ice bonding.

Keywords: glacial till, thawing process, shear behavior, strength properties, direct shear test

INTRODUCTION

Periglacial debris flow is an important surface process during deglaciation. Under a warming climate, Himalayan glaciers have decreased considerably in length and area, the largest are found in southeastern Tibet (Yao et al., 2012; Cui et al., 2018; Nie et al., 2021). Especially, climate warming affects not only accelerating the deglaciation processes but also increasing the mountain hazards risk. Climate waring induced a faster thawing process, where the amount of glacial meltwater can increase and then the catchments' hydrogeologic settings will be further changed. This thawing process is characterized by collapse and caving of glacial tills in steep alpine gullies, which can charge headwater catchments with loose sediments and become the source of labile materials for glacial debris flows (Huggel et al., 2012; Cossart et al., 2014; Wang et al., 2019). These sediments comprise mixtures of debris, ice, fluids, and other materials, and will deform and undergo a sudden loss of strength when subjected to freeze–thaw action (Viklander, 1998; Konrad, 2010;

Vanapalli and Han, 2016). The cause of frequent gully recharge remains unknown, although interactions between ice and soil particles should be taken as qualitative approximations of the soil mechanics of natural slopes.

There have been numerous studies on frozen permafrost. They propose that the presence of ice enhances soil mechanical properties, and ice debris mixtures deform little under low temperatures are generally more resistant than their components in alpine environments (Konrad and Morgenstern, 1980; Ting et al., 1983; Hivon and Sego, 1995). As temperature rises towards the thawing point, films of unfrozen water gradually form at the interface between ice and soil particles, glacial tills on the surface of steep slopes determines the evolution of slope collapse (Chamberlain et al., 1972; Zimmermann and Haeberli, 1992; Moore, 2014; Zhang et al., 2014). However, above findings are failure explain the conclusion that till provides the main source of materials for glacial debris flows.

Thawing can result in changes in internal friction angle and ice cohesion (Czurda and Hohmann, 1997; Lai et al., 2008). The decrease of cohesion with thawing is consistent with the exponential relationship between cohesion and ice content reported by Arenson and Springman (2005b). They focused on the effect of ice content on the cohesion of frozen soils at different temperatures, and did not study the effect of liquid water. However, after contact with water, glacial tills become extremely unstable and their compactness decreases (Vanapalli and Han, 2016). Both dry density and water content are key factors that affect till pore structure and particle distribution, which directly determine initial ice and water migration (Sayles and Carbee, 1981; Eskişar et al., 2015). Nevertheless, no consensus has been reached regarding the influence of thawing on soil mechanics; the relationship between ice phase transition and short-term soil instability remains unknown.

This study focuses on the shear and thawing processes, and further clarifies the contribution of ice bonding to shear strength. The objective of this study is to improve understanding of glacial debris flow initiation and sediment recharge in gullies by investigating the shear behavior and characteristics of frozen glacial tills after short periods of thawing. Glacial tills were collected from the headwater area of the Tianmo gully in Tibet. A total of 648 specimens with three different dry densities, three initial water contents, and 18 thawing times were subjected to conventional direct shear tests. Further, a quantitative assessment of the relationships among water content, dry density, total normal stress and thawing time were explored. More importantly, the potential relation between the ice particle characteristics and till strength to be discussed, and the mechanism variation of thawing on glacial till characteristics to be presented.

STUDY AREA AND SAMPLING LOCATION

Tianmo gully is in Parlung Tsangpo Basin on the southeastern Tibetan Plateau. The length of the main channel is approximately 5.1 km and the average gradient is 25.9% (King et al., 2016). The basin is wider upstream and narrower downstream. Tianmo gully is one of the tributaries of the Parlung Tsangpo River between the villages of Guxiang and Tongmai; the terrain is rugged and mountainous. Like most of the tributaries of the Parlung Tsangpo River in this area, Tianmo gully is short and steep; erosion rate is high and exceeds 5 mm per year (Wang et al., 2019). The headwater area of Tianmo gully is heavily glaciated (**Figures 1A,C,F** are the start and outlet points), and produces massive glacial tills at the front of the glaciers (Deng et al., 2017).

Assuming that the thickness of the ice debris cover is greater than that of the active layer of the permafrost, mass movement activity occurs only under specific topographic conditions and/or under the action of external meltwater sources or slope undercutting (Schomacker, 2008). However, there have been more than three large-scale debris flows took place in the Tianmo gully at July 25–31 (DF1) and September 5–8 (DF2) of 2010, September 4 of 2007 (DF3) (Ge et al., 2014), and all occurred during summer when temperature generally exceeded 25°C (**Figure 2**). In summer 2020, several fresh debris flows were found in the Tianmo gully (**Figure 1B**), which can be concluded that it is highly likely that thawing can initiate mass movement activity here. To better understand the mechanics of thawing glacial tills, samples were collected from the location shown in **Figure 1C**.
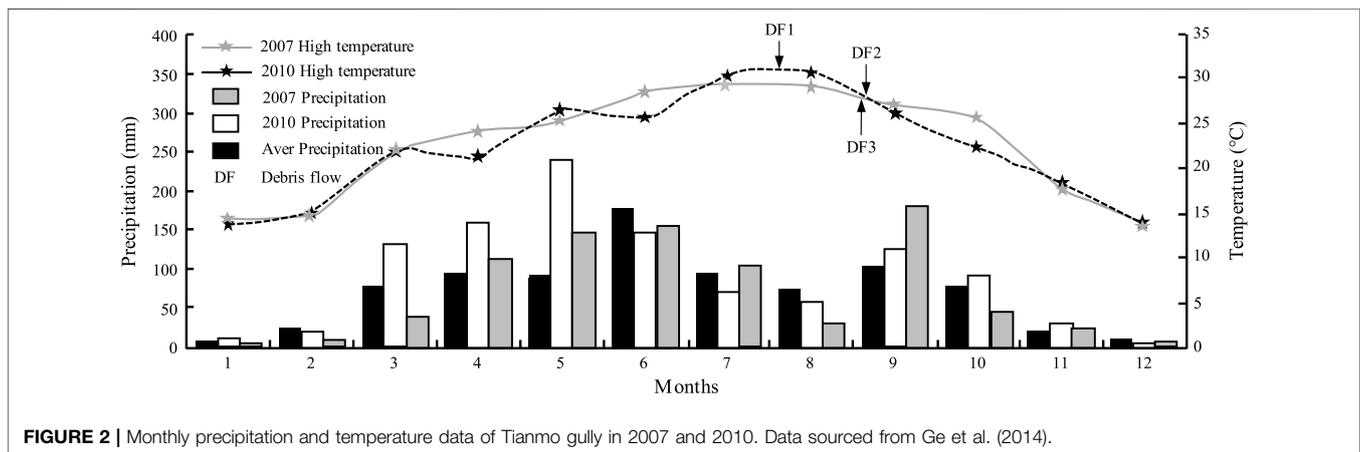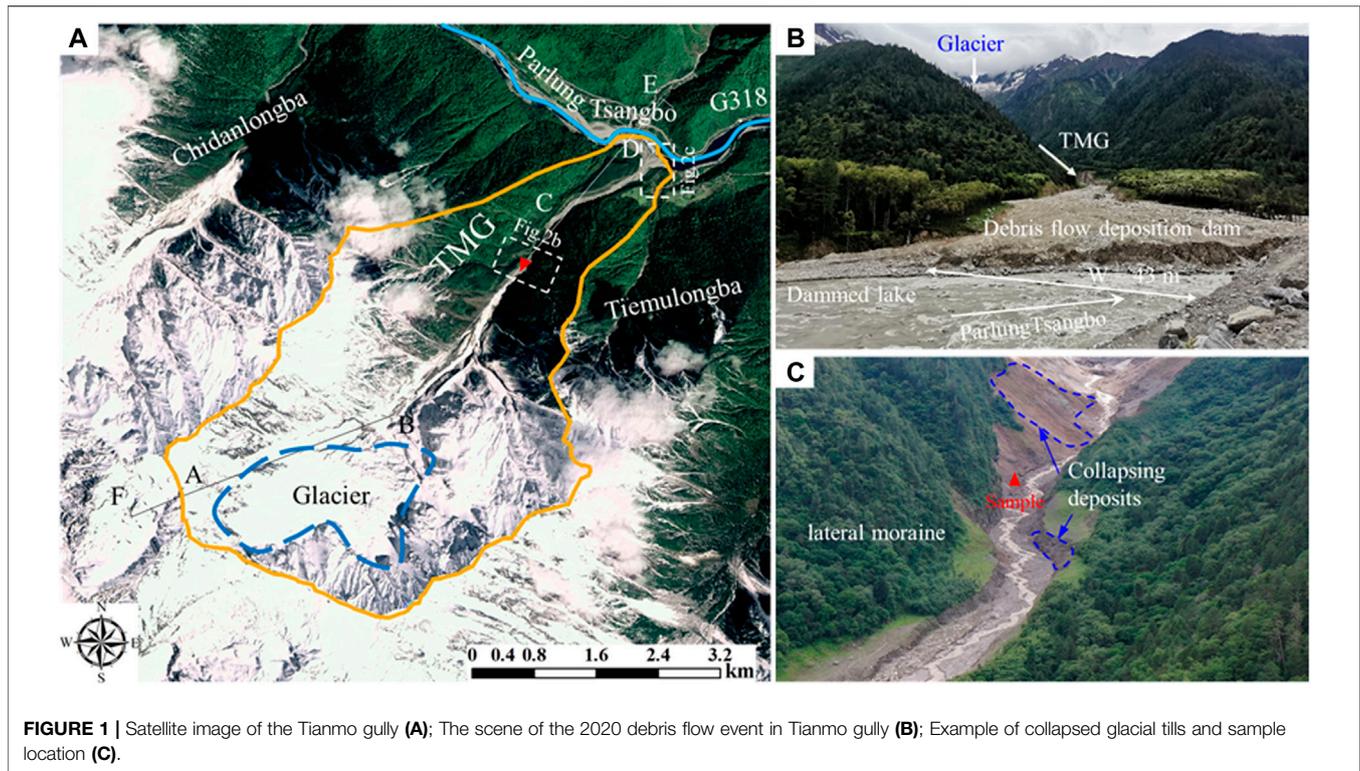
MATERIALS AND METHODS

Physical Properties of Glacial Tills

Sieves and a laser particle size analyzer were used to derive particle size distributions of the till samples. Samples contained poorly graded and sorted, among 24% gravel (4.5 mm $< d <$ 75 mm), 73% sand (0.075 mm $< d <$ 4.5 mm) with a small amount of silt ($d <$ 0.075 mm, nonplastic or very slightly plastic) and clay ($d <$ 0.075 mm, plastic) (ASTM, 2017); The uniformity coefficient (C_u = 21) and the coefficient of curvature (C_c = 0.57) were calculated (**Figure 3**). Other physical properties of the samples are shown in **Table 1**. It should be noted that the maximum dry density of samples is 2.03 g/cm³, the optimum water content is 8.03%, these values were derived from soil compaction tests which can present different soil properties.

Specimen Preparation

Soil samples were placed in an incubator at 105°C for 6 h. The shear test specimens were prepared with diameters of 61.8 mm and heights of 20 mm. Because the range and size of maximum particle diameters should remain below a 10th of specimen diameter, soil particles were redistributed following the similarity principle of dimensional analysis, samples were passed through a 2 mm standard sieve. (ASTM, 2017). Glacial till samples were prepared and spread evenly on a plastic plate, they were sprayed with de-aired water to increase their gravimetric water contents to the target values (i.e., 8, 12 and 16%, were approached the optimum water content, plastic limit and liquid limit respectively). where the mixtures were kept 1 day for moisture equalization. To obtain uniform specimens, the

FIGURE 1 | Satellite image of the Tianmo gully **(A)**; The scene of the 2020 debris flow event in Tianmo gully **(B)**; Example of collapsed glacial tills and sample location **(C)**.

FIGURE 2 | Monthly precipitation and temperature data of Tianmo gully in 2007 and 2010. Data sourced from Ge et al. (2014).

static compaction method was used, the each of the soil specimens were compacted in four layers using a mold. The target dry density of each specimen is 1.70, 1.85 and 2.00 g/cm^3 (it's bound by the maximum dry density), more details are given in **Table 2**.

Water can freeze into solid state (ice) at standard atmospheric pressure when the temperature is at 0 °C. Based on the filed investigations and monitoring, the air temperature in high mountain aeras can decrease with elevation at rate of 0.54°C per 100 m (Deng et al., 2017; Wei et al., 2017). Considering the purpose of the present study, the freezing temperature was selected at –15°C for 24 h

to ensure that the water in all samples can be froze. Based on temperature of debris flows (**Figure 2**), the temperature of thawing phase of experiment were set 25°C. On the basis of their study of frozen soil specimens, Fu et al. (2021) reported that specimen diameters remained unchanged and all ice had completely converted to liquid water after 4 h of thawing. Therefore, complete thawing was assumed that after 4 h, and used increments of 0.25 h between 0 and 4 h to represent different phases of thawing ($t = 0, 0.25, \ldots, 3.75, 4$ h). Specimens at $t = *$ were not subjected to freeze–thaw action. **Table 2** shows thawing times and preparation details of 18 groups of specimens ($t = *, 0, 0.25, \ldots, 3.75, 4$ h).
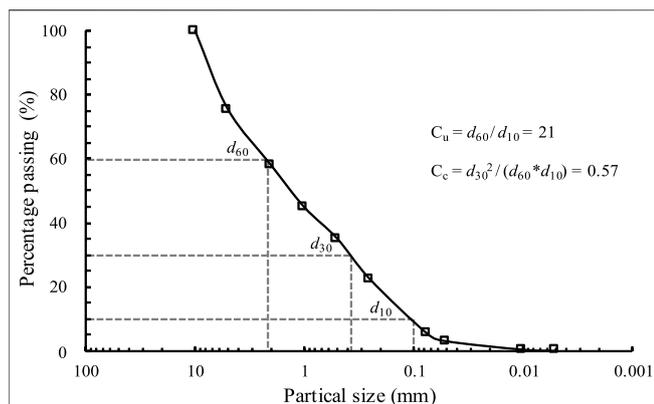
FIGURE 3 | Particle size distributions of glacial till samples.

$C_u = d_{60}/d_{10} = 21$

$C_c = d_{30}^2/(d_{60} * d_{10}) = 0.57$

Direct Shear Tests Plan

Direct shear tests are commonly used to measure soil shear strength. Compared with triaxial tests, direct shear tests can achieve failure in frozen samples in considerably less time (Gan et al., 1988). According to the filed investigations, glacial tills wasting processes are demonstrated to rapid loading/shearing conditions, and the potential water could not immediately move from the sediments. Therefore, the undrained test was normally selected to study the shear behavior in laboratory (Nickling and Bennett, 1984; Wang et al., 2007). To measure uniform residual strength, all shear tests were terminated when horizontal displacement reached 10 mm at a shear rate of 2.4 mm per minute (Jewell, 1989). Considering the glacial tills may fail at different shallow depths (several meters) due to freezing-thawing effects (Ferrick et al., 2005; Kos et al., 2016), four normal stresses (i.e., 50, 100, 150 and 200kPa) were selected to examine the shear behavior and then to determine the strength profile. A total of 648 specimens were tested. Details of the tests and shear strength of the specimens are shown in **Table 2**.

Parameters Characterizing Shear Behavior

Shear tests were performed on till specimens to investigate the effect of thawing time on shear behavior and variations of shear strength and deformation. Stress–strain curves provide important information for the evaluation of till shear behavior, instability, failure and deformation modes (Ling et al., 2007). The peak stress (τ_r), residual stress (τ_r), cohesion (C), and internal friction angle (φ) were measured. The initial elastic modulus (K_i) was used to characterize the stage of shear stress growth (between $\tau = 0$ and

$\tau = \tau_p$), and the softening index (I_B) was used to characterize the strain softening that occurred between $\tau = \tau_p$ and $\tau = \tau_r$. Between $\tau = 0$ and $\tau = \tau_0$, the relationship between shear stress and horizontal displacement was linear and the specimen underwent approximately elastic deformation. To characterize the stage of elastic deformation, the elastic coefficient K_i was used, which is the ratio between the initial shear stress at the end of this stage (τ_0) and the corresponding horizontal displacement increment (Δx_0):

$$K_i = \frac{\tau_0}{\Delta x_0} \qquad (1)$$

The difference between peak strength and residual strength $(\tau_p - \tau_r)$ was used to characterize the stage of plastic deformation, and the softening coefficient I_B to characterize the softening characteristics of the shear process (Yang and Wei 2012):

$$I_B = \frac{\tau_p - \tau_r}{\tau_p} \qquad (2)$$

As seen in **Eq. (2)**, if there is a peak stress (τ_p), the range of I_B is between 0 and 1, and the larger the I_B, the more pronounced the softening after the peak.

RESULTS

Shear Behavior and Thawing Time

For all specimens, horizontal displacement (Δx) was less than 3 mm at peak stress and the stage of uniform $\tau_p - \tau_r$ was reached before the end of the tests. A group of samples with same physical state $(\rho_d = 2.0 \text{ g/cm}^3, w = 8\%)$ was selected, shear behavior as shown in **Figure 4**. Specimens with thawing time of $t = 0$ h softened and contracted considerably; shear strength was considerably lower in specimens with $t = 4$ h; the largest reduction in shear strength was found in specimens with $t = 2$ h. Peak stress to displacement ratio (τ/σ) was largest for specimens with $t = 0$ h (0.857), and smaller for specimens with $t = 2$ h (0.716), $t = 4$ h (0.745), and $t = {}^\star$ (0.776). These results show that the shear behavior of glacial tills subjected to freeze–thaw action is different from the behavior of tills that have not been subjected to freeze–thaw, which is in agreement with the results of Ferrick and Gatto (2005). More interesting is that our results indicate the shear behavior of glacial tills is affected by thawing time which provides direct experimental evidence for the influence of solid ice on the shear behavior of soil samples.

There were considerable variations of K_i and I_B with thawing time; five phases can be identified from **Figure 5** (Condition of
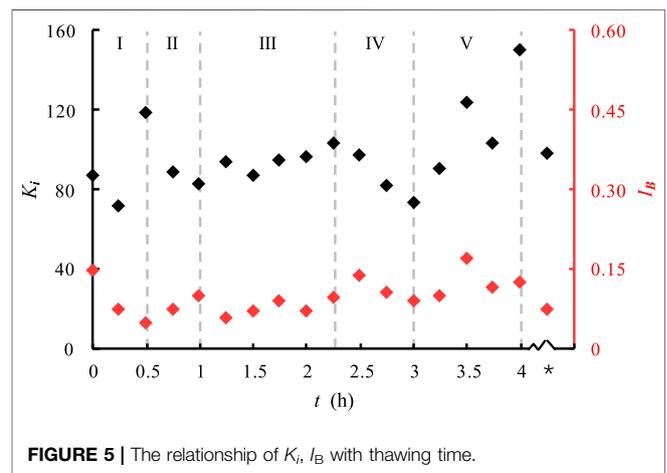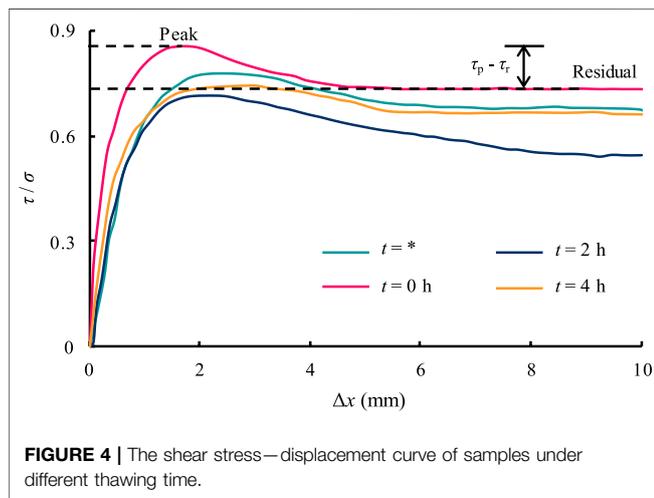
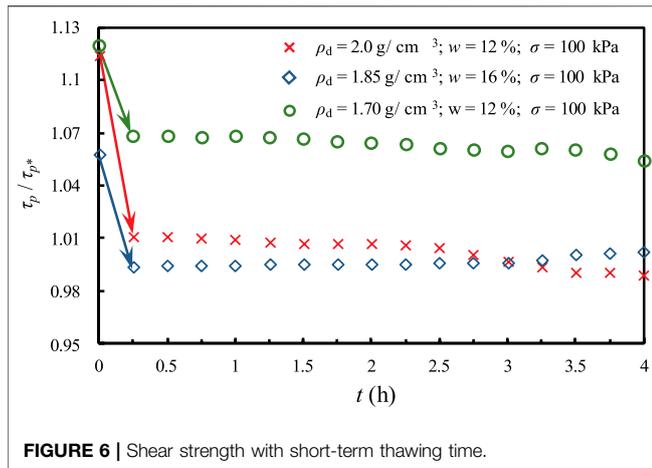**TABLE 1 |** Physical properties of glacial till samples.

Index	Specific gravity Gs	Maximum dry density ρ_d (g/cm³)	Optimum water content w_{opt} (%)	Liquid limit w_l (%)	Plastic limit w_P (%)	Plastic index I_P
value	2.78	2.03	8.03	16.40	12.07	4.33

TABLE 2 | Program and result of direct shear test on glacial till specimens.

Group no	Soil sample no	ρ_d (g/cm³)	w (%)	Specimen preparation	c (kPa)	φ (°)
1	$G^*_1\text{-}w_8$	1.70	8	Without freezing treatment, used for References	0.13	32.14
	$G^*_1\text{-}w_{12}$		12		0.36	31.73
	$G^*_1\text{-}w_{16}$		16		0.54	33.46
	$G^*_2\text{-}w_8$	1.85	8		0.65	32.69
	$G^*_2\text{-}w_{12}$		12		0.72	34.23
	$G^*_2\text{-}w_{16}$		16		0.87	35.27
	$G^*_3\text{-}w_8$	2.00	8		1.29	36.68
	$G^*_3\text{-}w_{12}$		12		1.52	35.83
	$G^*_3\text{-}w_{16}$		16		1.22	35.93
2	$G^0_1\text{-}w_8$	1.70	8	Frozen at -15 °C for 12 h without melting, represents frozen state	5.02	30.09
	$G^0_1\text{-}w_{12}$		12		6.90	29.52
	$G^0_1\text{-}w_{16}$		16		8.58	30.55
	$G^0_2\text{-}w_8$	1.85	8		8.64	30.74
	$G^0_2\text{-}w_{12}$		12		10.00	32.17
	$G^0_2\text{-}w_{16}$		16		10.82	32.73
	$G^0_3\text{-}w_8$	2.00	0		9.75	34.83
	$G^0_3\text{-}w_{12}$		12		8.90	33.78
	$G^0_3\text{-}w_{16}$		16		10.70	33.57
3–18	$G^{0.25}_1\text{-}w_8 \sim G^4_1\text{-}w_8$	1.70	8	Frozen at -15 °C for 12 h, and melted at 24 °C for 0.25–4 h, represents partly frozen state	2.94–0.13	30.49–32.15
	$G^{0.25}_1\text{-}w_{12} \sim G^4_1\text{-}w_{12}$		12		4.41~0.36	30.19~31.74
	$G^{0.25}_1\text{-}w_{16} \sim G^4_1\text{-}w_{16}$		16		5.86~0.54	31.29–33.48
	$G^{0.25}_2\text{-}w_8 \sim G^4_2\text{-}w_8$	1.85	8		6.23~0.66	31.10–32.71
	$G^{0.25}_2\text{-}w_{12} \sim G^4_2\text{-}w_{12}$		12		7.79~0.72	32.68–34.29
	$G^{0.25}_2\text{-}w_{16} \sim G^4_2\text{-}w_{16}$		16		8.52~0.87	33.44–35.28
	$G^{0.25}_3\text{-}w_8 \sim G^4_3\text{-}w_8$	2.00	8		7.50~1.30	35.12–36.72
	$G^{0.25}_3\text{-}w_{12} \sim G^4_3\text{-}w_{12}$		12		6.54~1.53	34.24–35.86
	$G^{0.25}_3\text{-}w_{16} \sim G^4_3\text{-}w_{16}$		16		7.31~1.23	34.26–35.95

$G^t_{\rho d}$: glacial tills, subscript represents dry density, superscript represents melting time (* refers to non-freeze-thaw samples), t: short-term thawing time; ρ_d: dry density; w: initial water content of sample preparation; c: Cohesion; φ: Internal friction angle.

FIGURE 4 | The shear stress—displacement curve of samples under different thawing time.

FIGURE 5 | The relationship of K_i, I_B with thawing time.

FIGURE 6 | Shear strength with short-term thawing time.

the samples: $\rho_d = 1.85$ g/cm^3, $w = 16\%$, $\sigma = 100$ kPa). Using K_i as a measure of the resistance of specimens to elastic deformation, a large K_i indicates high stiffness and large variations of shear stress per unit horizontal displacement increment. In stage I, the ability of glacial tills to resist elastic deformation increases with the decrease of ice content because solid ice prevents the specimen from recovering from deformation. For stages I, III, IV and V, the relationship between I_B and t and that between K_i and t follow similar trends. Softening was minimal for specimens with $t = 0.5$ h, which implies the movement of ice particles into the soil skeleton during initial thawing; as a result, the structure of the specimens becomes more unstable. These findings suggest that the shear behavior of thawing samples is affected by the combined action of ice and water and varies with thawing time.

Using experimental results, the hypothesis is tested that shear behavior of specimens with $t = 4$ h is similar to that of specimens that have not been subjected to freeze–thaw action ($t = {}^{*}$). One possible reason is that solid ice affects the arrangement of soil particles. Specimens that are subjected to freeze–thaw action are more compact at the early stage of loading, and are therefore more resistant to shear. However, under freeze–thaw action, solid ice forms and disappears rapidly. As a result, the arrangement of soil particles within the specimens become more random (Atkinson and Little, 1988) and specimens become less resistant to shear deformation as loading continues and shear stress increases.

Relationship Between Peak Strength and Thawing Time

The variation of the strength of thawing soil samples can be considered as a quasi-dynamic transition. As shown in **Figure 6**, the variation of τ_p/τ_{p*} with thawing time for the different series of experiments. Peak strengths of specimens not subjected to freeze–thaw action (τ_{p*}) were used as the reference value, and our main observations are as follows:

a) Peak shear strengths of specimens with $t = 0$ h were considerably higher than peak shear strengths of specimens

with any other thawing time. This indicates that high ice content was associated with high shear strength.

b) Shear strengths of specimens with $t = 0.25$ h were considerably lower than those of specimens with $t = 0$ h. Specimens with $t = 0.25$–4 h had similar peak strengths. This indicates that thawing of solid ice at the beginning of the thawing process is the key factor that controls peak strengths; its impact on peak strength is greater than the combined impact of loading and the physical characteristics of the specimen.

c) Peak strengths decreased with increasing thawing time for some specimens with $t \geq 0.25$ h, and increased with increasing thawing time in others. This suggests that the shear strength of thawing specimens is not controlled by a single universal factor.

To examine the effects of different stages of thawing on the attainable shear strength of glacial tills, thawing time as a quantitative test was used control to represent different stages of thawing and also of the transformation of solid ice. It is shows that the relationship between peak strength and thawing time at initial thawing stage is little or not affected independent of loading conditions and the physical characteristics of the specimens.

However, these results show that except for the initial thawing stage, shear strength at different thawing times may be controlled by dry density and water content. Water content (w) is a measure of the liquid water content of ice particles and dry density (ρ_d) is a measure of the water channels in the thawing specimen (Ladanyi and Morel, 1990). As shown in **Figure 7**, it normalized total normal stress, the relationship between shear strength and dry density and water content of unthawed ($t = 0$ h) and thawed state ($t = 4$ h) is presented. For unthawed specimens ($t = 0$ h), peak strength increased with increasing w for specimens with ρ_d of 2.00 g/cm^3, and decreased with increasing w for specimens with ρ_d of 1.70 and 1.85 g/cm^3. However, for all thawed specimens ($t = 4$ h), peak strengths decreased with increasing w. It can be found that the shear strength decreases with the increase of water content when the dry density is 2.00 g/cm^3 in both states.

FIGURE 7 | Effect of dry density and water content on shear strength under different thawing conditions.
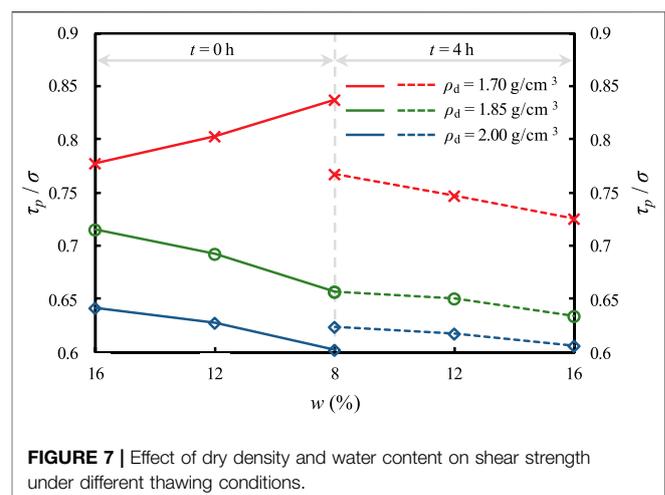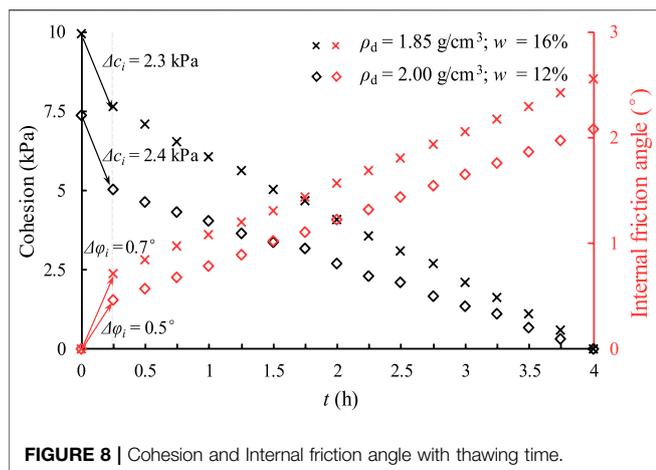
FIGURE 8 | Cohesion and Internal friction angle with thawing time.

Hence, the amount of contact between soil particles is determined by dry density and affects the bonding of solid ice. In addition, further analysis of the variation trend of ρ_d at 1.70 and 1.85 g/cm^3 in $t = 0$ h and $t = 4$ h can be obtained the shear strength of frozen soils can be increased by increasing initial water content in loose soils. It's not hard to understand there is little or no water transfer within the internal pore structure of frozen samples theoretically (Burt and Williams, 1976), which can be inferred the looser the soil sample, the greater the effect of solid ice.

Effect of Short-Term Thawing on Shear Strength

In addition to shear strength, other parameters are needed to characterize soil shear behavior (Arenson and Springman, 2005a). While experiments have established the effect of solid ice on shear strength, the effects of cohesion 3) and internal friction angle (φ) on shear strength are less clear. In thawing soils, the relationship between peak stress, cohesion, normal stress and angle of friction are as follows:

$$\tau_p = c - \sigma \tan \varphi \tag{3}$$

There are also films of unfrozen water in the soil (Chamberlain and Gow, 1979); therefore, the cohesion (c_i) and internal friction angle (φ_i) exerted by solid ice at different thawing times can be rewritten as:

$$c_{ik} = c_k - c_* \tag{4}$$

$$\varphi_{ik} = \varphi_k - \varphi_0 \tag{5}$$

where c_* is the cohesion of the soil sample itself, φ_0 refers to the internal friction of the sample before thawing (i.e., $t = 0$ h), and $k = 1, 2, \ldots, 17, 18$ corresponds to $t_i = 0\,h, 0.25\,h, \ldots, 3.75\,h, 4\,h$; c_* represents the unique condition of each frozen soil sample.

Cohesion is the shear strength without any normal stress on the shear failure surface and is the result of the combined action of gravitational attraction and repulsion between soil particles (Seo et al., 2004). Glacial tills have the characteristics of sand; they generally have no cohesion or a weak false cohesive force (Zhou et al., 2019). However, the black

symbols in **Figure 8** indicate that the highest c_i was reached at 9.95 kPa and $t = 0$ h. Cementation ice formed by *in situ* freezing of liquid water can significantly increase the proportion of cohesive strength in the shear strength of frozen glacial till specimens (Sterpi, 2015). Moreover, for specimens with $t \geq 0.25$ h, c_i decreased linearly with increasing thawing time.

The red symbols in **Figure 9** indicate the variation of internal friction angle with thawing time. Least square linear regression shows that, for specimens with $t \geq 0.25$ h, φ_i increased linearly with thawing time; this result is consistent with the findings of Nater et al. (2015). However, liquid water reduces the friction between soil particles, and an exponential relationship between the internal friction angle and ice content ignores the effect of films of unfrozen water on the friction between soil particles.

For specimens with $t = 0.25$ h (gray dashed line in **Figure 8**), maximum friction was 2.58°, which was far below the value of cohesion. This suggests that the effects of frozen water and ice on cohesion are stronger at the initial phase of thawing, and that the effect of ice on soil friction and cohesion is stronger in loose soils.
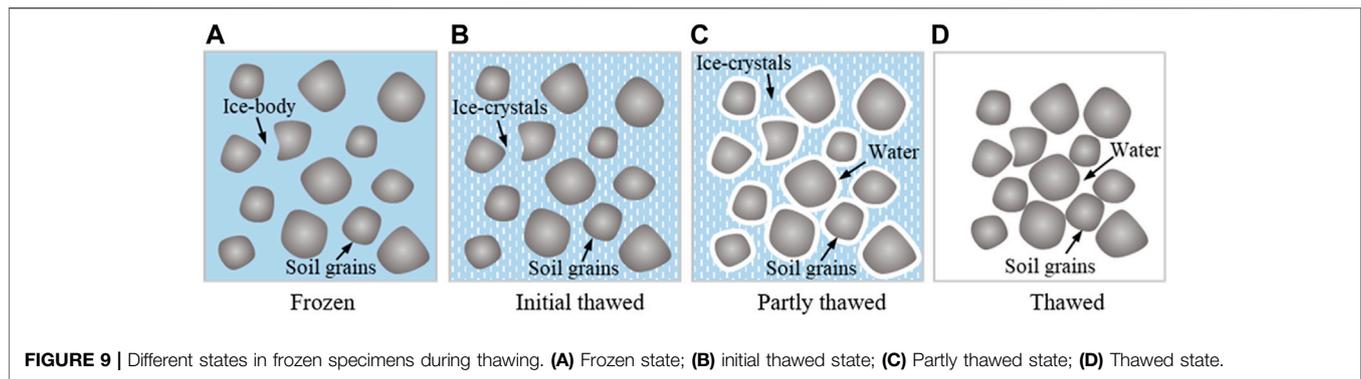
These results show that the cohesion of glacial till specimens decreases considerably with increasing thawing time. They support the hypothesis that the self-perpetuating destruction of thawing soils depends on the short-term destruction of ice bonding (Arenson and Springman, 2005a). This mechanism could explain the frequent sediment recharge of gullies, although interactions between ice and soil particles can only be used as qualitative approximations of the soil mechanics of natural slopes.

DISCUSSION

Shear strength of thawing soils indicate that thawing evolves with time. Therefore, it is necessary to examine the mechanisms of phase transformation of solid ice. Unfrozen water, ice, and frozen water change phase as temperature reaches the melting point. **Figure 9** shows the four typical states of thawing soils.

In frozen soils, individual soil grains may not be in contact with one other (**Figure 9A**). The main form of ice is the ice body; it has a relatively stable structure because of the tetrahedral arrangement of molecules (Liu and Peng, 2009). The soil skeleton comprises the ice body and soil grains, which increase shear resistance (Özgan et al., 2015). Friction contributes little to shear resistance, and shear strength mainly comes from cohesion. The experimental results show that the largest amount of softening and the highest peak strength occurred in specimens with $t = 0$ h (**Figure 4**); this could be an explanation of the control of shear resistance and strength of frozen soils by cohesion at the particle scale.

After initial thawing, ice volume decreases; the ice body transforms into ice crystals with broken hydrogen bonds between the ice molecules; liquid water is absent (**Figure 9B**). The soil skeleton is ruptured and reduced in volume. Soil grains are in contact with ice crystals. Friction increases while cohesive bonding decreases; there are large increases in internal friction angle and large decreases in cohesion (**Figure 8**). The ice body and soil particles form an integrated whole, which has a higher resistance to deformation

FIGURE 9 | Different states in frozen specimens during thawing. **(A)** Frozen state; **(B)** initial thawed state; **(C)** Partly thawed state; **(D)** Thawed state.

than soils comprising ice crystals and soil particles (Ewertowski and Tomczyk, 2015). During this stage, the ice body transforms into ice crystals in discrete steps, and soil structure is unstable.

In partly thawed soils, both ice crystals and unfrozen water are present in the voids between particles; soil grains are surrounded by films of unfrozen water, which are in contact with one another (**Figure 9C**) (Arenson and Springman, 2005a). Ice molecules break apart to form water substructures with reduced order. Ice bonding weakens and lubrication by liquid water increases; as a result, cohesion decreases and granular friction increases. Partly thawed soils have increased shear resistance and the corresponding horizontal displacement under a given level of stress also increases (i.e., shear behavior at $t = 2$ h in **Figure 4**).

In thawed soils, all pore water is in the liquid phase and ice is absent (**Figure 9D**) (Ladanyi and Morel, 1990); there is little order in the spatial distribution of water molecules, and is similar to the arrangement of any conventional unfrozen soils (Fredlund et al., 1978). However, thawed soils also differ from unfrozen soils; the transition from frozen to thawed soil changes pore structure, and allows full contact between soil grains (Nater et al., 2015). Over the long term, ice bonding completely disappears from drained thawed soils. Glacial tills are widely distributed in alpine environments. Therefore, it is likely that there is zero cohesion in drained soils under extremely high temperatures. Moreover, a larger sliding friction is needed to resist shear deformation and gives rise to a peak internal friction angle (**Figure 8**).

The thawing of frozen soils typically includes the breaking up of the ice body, thawing of ice crystals, formation of films of unfrozen water, and contact between soil grains facilitated by liquid water. This process gives rise to the shear deformation of the glacial till specimens that was observed in our experiments. The morphological changes and phase transformation of solid ice affect the mechanical behavior of thawing soils over time. The amount of solid ice decreases and the amount of liquid water increases with increasing thawing time and affect shear strength. Changes in cohesion and friction vary with thawing time.

CONCLUSION

In this study, the experiments were conducted to examin the role of thawing on the mechanical properties of glacial tills.

Direct shear tests were performed on till specimens with three different dry densities and three different initial water contents after 18 thawing times. Our primary findings are as follows:

a) Shear softening decreases with increasing thawing time. The difference between peak and critical resistances decreases with increasing thawing time and reflects changes in shear behavior. Dry density can enhance shear strength. However, in soils with high density, initial water content may result in the decrease of shear strength.

b) Shear strength decreases considerably after initial thawing time. Decrease is larger in soils with higher initial water content. For loose soils, shear strength increases with increasing initial water content.

c) In accordance with the Mohr–Coulomb theory, the internal friction angle increases and cohesion decreases with increasing thawing time. This indicates that the cemented ice formed by *in situ* freezing of water can significantly improve the cohesive component of the shear strength of frozen soils.

d) Completely frozen soils are more stable than partly thawed or unfrozen soils. Partly thawed soils are less stable than frozen or unfrozen soils because they are made up of ice crystals that have low resistance to deformation. This analysis depicted changes in ice and intergranular contact modalities and mechanisms with thawing time, and provides a useful framework to understand variations in the shear behavior of glacial tills.

DATA AVAILABILITY STATEMENT

The raw data supporting the conclusion of this article will be made available by the authors, without undue reservation.

AUTHOR CONTRIBUTIONS

YF performed the tests and wrote this manuscript. YJ contributed to the conceptualization, supervision and funding acquisition. JW carried out the field investigation. ZL and XL reviewed and edited

the manuscript. All authors listed have contributed sufficiently to the project to be included as authors, and all those who are qualified to be authors are listed in the author byline.

REFERENCES

Arenson, L. U., and Springman, S. M. (2005a). Mathematical Descriptions for the Behaviour of Ice-Rich Frozen Soils at Temperatures Close to 0 °C. *Can. Geotech. J.* 42 (2), 431–442. doi:10.1139/t04-109

Arenson, L. U., and Springman, S. M. (2005b). Triaxial Constant Stress and Constant Strain Rate Tests on Ice-Rich Permafrost Samples. *Can. Geotech. J.* 42 (2), 412–430. doi:10.1139/t04-111

ASTM (2017). *Standard Practice for Classification of Soils for Engineering Purposes (Unified Soil Classification System)*. ASTM standard D2487- 17. West Conshohocken, Pennsylvania: American Society for Testing Materials.

Atkinson, J. H., and Little, J. A. (1988). Undrained Triaxial Strength and Stress-Strain Characteristics of a Glacial till Soil. *Can. Geotech. J.* 25 (3), 428–439. doi:10.1139/t88-048

Burt, T. P., and Williams, P. J. (1976). Hydraulic Conductivity in Frozen Soils. *Earth Surf. Process.* 1 (4), 349–360. doi:10.1002/esp.3290010404

Chamberlain, E., Groves, C., and Perham, R. (1972). The Mechanical Behaviour of Frozen Earth Materials under High Pressure Triaxial Test Conditions. *Géotechnique* 22 (3), 469–483. doi:10.1680/geot.1972.22.3.469

Chamberlain, E. J., and Gow, A. J. (1979). Effect of Freezing and Thawing on the Permeability and Structure of Soils. *Eng. Geology.* 13 (14), 73–92. doi:10.1016/b978-0-444-41782-4.50012-9

Cossart, E., Mercier, D., Decaulne, A., Feuillet, T., Jónsson, H. P., and Saemundsson, Þ. (2014). Impacts of post-glacial Rebound on Landslide Spatial Distribution at a Regional Scale in Northern Iceland (Skagafjörður). *Earth Surf. Process. Landforms* 39 (3), 336–350. doi:10.1002/esp.3450

Cui, P., Deng, H.-Y., Wang, C.-H., et al. (2018). *Mountain Hazards*. Beijing, China: Higher Education Press, pp189–216. (In Chinese).

Czurda, K. A., and Hohmann, M. (1997). Freezing Effect on Shear Strength of Clayey Soils. *Appl. Clay Sci.* 12 (1-2), 165–187. doi:10.1016/s0169-1317(97) 00005-7

Deng, M., Chen, N., and Liu, M. (2017). Meteorological Factors Driving Glacial till Variation and the Associated Periglacial Debris Flows in Tianmo Valley, South-Eastern Tibetan Plateau. *Nat. Hazards Earth Syst. Sci.* 17 (03), 345–356. doi:10.5194/nhess-17-345-2017

Eskişar, T., Altun, S., and Kalıpcılar, İ. (2015). Assessment of Strength Development and Freeze-Thaw Performance of Cement Treated Clays at Different Water Contents. *Cold Regions Sci. Tech.* 111 (mar), 50–59. doi:10.1016/j.coldregions.2014.12.008

Ewertowski, M. W., and Tomczyk, A. M. (2015). Quantification of the Ice-Cored Moraines' Short-Term Dynamics in the High-Arctic Glaciers Ebbabreen and Ragnarbreen, Petuniabukta, Svalbard. *Geomorphology* 234 (apr.1), 211–227. doi:10.1016/j.geomorph.2015.01.023

Ferrick, M. G., and Gatto, L. W. (2005). Quantifying the Effect of a Freeze-Thaw Cycle on Soil Erosion: Laboratory Experiments. *Earth Surf. Process. Landforms* 30 (10), 1305–1326. doi:10.1002/esp.1209

Fredlund, D. G., Morgenstern, N. R., and Widger, R. A. (1978). The Shear Strength of Unsaturated Soils. *Can. Geotech. J.* 15 (3), 313–321. doi:10.1139/t78-029

Fu, Y., Liu, Z., and Jiang, Y. (2021). *Effect of Short-Term Thawing on the Mechanical Properties of Frozen Glacial Tills, EGU General Assembly, Online, 19-30 Apr 2021*. doi:10.5194/egusphere-egu21-12139

Gan, J. K. M., Fredlund, D. G., and Rahardjo, H. (1988). Determination of the Shear Strength Parameters of an Unsaturated Soil Using the Direct Shear Test. *Can. Geotech. J.* 25 (3), 500–510. doi:10.1139/t88-055

Ge, Y. G., Cui, P., Su, F. H., Zhang, J. Q., and Chen, X. Z. (2014). Case History of the Disastrous Debris Flows of Tianmo Watershed in Bomi County, Tibet, China: Some Mitigation Suggestions. *J. Mountain Sci.* 11 (05), 1253–1276. doi:10.1007/s11629-014-2579-2

Hivon, E. G., and Sego, D. C. (1995). Strength of Frozen saline Soils. *Can. Geotech. J.* 32 (2), 336–354. doi:10.1139/t95-034

Huggel, C., Clague, J. J., and Korup, O. (2012). Is Climate Change Responsible for Changing Landslide Activity in High Mountains? *Earth Surf. Process. Landforms* 37 (1), 77–91. doi:10.1002/esp.2223

Jewell, R. A. (1989). Direct Shear Tests on Sand. *Géotechnique* 39 (2), 309–322. doi:10.1680/geot.1989.39.2.309

King, G. E., Herman, F., and Guralnik, B. (2016). Northward Migration of the Eastern Himalayan Syntaxis Revealed by OSL Thermochronometry. *Science* 353 (6301), 800–804. doi:10.1126/science.aaf2637

Konrad, J.-M. (2010). Hydraulic Conductivity Changes of a Low-Plasticity till Subjected to Freeze-Thaw Cycles. *Géotechnique* 60 (09), 679–690. doi:10.1680/geot.08.P.020

Konrad, J.-M., and Morgenstern, N. R. (1980). A Mechanistic Theory of Ice Lens Formation in fine-grained Soils. *Can. Geotech. J.* 17 (04), 473–486. doi:10.1139/t80-056

Kos, A., Amann, F., Strozzi, T., Delaloye, R., Ruette, J., and Springman, S. (2016). Contemporary Glacier Retreat Triggers a Rapid Landslide Response, Great Aletsch Glacier, Switzerland. *Geophys. Res. Lett.* 43 (24), 12466–12474. doi:10.1002/2016GL071708

Ladanyi, B., and Morel, J.-F. (1990). Effect of Internal Confinement on Compression Strength of Frozen Sand. *Can. Geotech. J.* 27 (1), 8–18. doi:10.1139/t90-002

Lai, Y., Li, S., Qi, J., Gao, Z., and Chang, X. (2008). Strength Distributions of Warm Frozen clay and its Stochastic Damage Constitutive Model. *Cold Regions Sci. Tech.* 53 (2), 200–215. doi:10.1016/j.coldregions.2007.11.001

Ling, H.-I., Callisto, L., Leshchinsky, D., and Koseki, J. (2007). Soil Stress-Strain Behavior: Measurement, Modeling and Analysis. *Solid Mech. Its Appl.* 146 (5), 83–93. doi:10.1007/978-1-4020-6146-2

Liu, J.-K., and Peng, L.-Y. (2009). Experimental Study on the Unconfined Compression of a Thawing Soil. *Cold Regions Sci. Tech.* 58 (1-2), 92–96. doi:10.1016/j.coldregions.2009.03.008

Moore, P. L. (2014). Deformation of Debris-Ice Mixtures. *Rev. Geophys.* 52 (3), 435–467. doi:10.1002/2014rg000453

Nater, P., Arenson, L. U., and Springman, S. M. (2015). *Choosing Geotechnical Parameters for Slope Stability Assessments in Alpine Permafrost Soils*. Alaska, America: Ninth International Conference on Permafrost, 1260–1266.

Nickling, W. G., and Bennett, L. (1984). The Shear Strength Characteristics of Frozen Coarse Granular Debris. *J. Glaciol.* 30 (106), 348–357. doi:10.1017/S0022143000000620110.3189/s0022143000006201

Nie, Y., Pritchard, H. D., Liu, Q., Hennig, T., Wang, W., Wang, X., et al. (2021). Glacial Change and Hydrological Implications in the Himalaya and Karakoram. *Nat. Rev. Earth Environ.* 2, 91–106. doi:10.1038/s43017-020-00124-w

Özgan, E., Serin, S., Ertürk, S., and Vural, I. (2015). Effects of Freezing and Thawing Cycles on the Engineering Properties of Soils. *Soil Mech. Found. Eng.* 52 (2), 95–99. doi:10.1007/s11204-015-9312-1

Sayles, F. H., and Carbee, D. L. (1981). Strength of Frozen silt as a Function of Ice Content and Dry Unit Weight. *Eng. Geology.* 18 (1-4), 55–66. doi:10.1016/0013-7952(81)90046-6

Schomacker, A. (2008). What Controls Dead-Ice Melting under Different Climate Conditions? A Discussion. *Earth-Science Rev.* 90 (3-4), 103–113. doi:10.1016/j.earscirev.2008.08.003

Seo, M. W., Park, I. J., and Park, J. B. (2004). Development of Displacement-Softening Model for Interface Shear Behavior between Geosynthetics. *Soils and Foundations* 44 (6), 27–38. doi:10.3208/sandf.44.6_27

Sterpi, D. (2015). Effect of Freeze-Thaw Cycles on the Hydraulic Conductivity of a Compacted Clayey silt and Influence of the Compaction Energy. *Soils and Foundations* 55 (5), 1326–1332. doi:10.1016/j.sandf.2015.09.030

Ting, J. M., Torrence Martin, R., and Ladd, C. C. (1983). Mechanisms of Strength for Frozen Sand. *J. Geotech. Engrg.* 109 (10), 1286–1302. doi:10.1061/(asce)0733-9410(1983)109:10(1286)

Vanapalli, S. K., and Han, Z. (2016). Modelling the Mechanical Properties of a Compacted Glacial till. *Indian Geotech J.* 46 (3), 261–271. doi:10.1007/s40098-016-0183-9

Viklander, P. (1998). Permeability and Volume Changes in till Due to Cyclic Freeze-Thaw. *Can. Geotechnical J.* 35 (03), 471–477. doi:10.1139/cgj-35-3-47110.1139/t98-015

Wang, H., Cui, P., Liu, D., Liu, W., Bazai, N. A., Wang, J., et al. (2019). Evolution of a Landslide-Dammed lake on the southeastern Tibetan Plateau and its Influence on River Longitudinal Profiles. *Geomorphology* 343, 15–32. doi:10.1016/j.geomorph.2019.06.023

Wang, J., Dove, J. E., and Gutierrez, M. S. (2007). Discrete-continuum Analysis of Shear Banding in the Direct Shear Test. *Géotechnique* 57 (6), 513–526. doi:10.1680/geot.2007.57.6.513

Wei, R., Zeng, Q., Davies, T., Yuan, G., Wang, K., Xue, X., et al. (2018). Geohazard cascade and Mechanism of Large Debris Flows in Tianmo Gully, SE Tibetan Plateau and Implications to hazard Monitoring. *Eng. Geology.* 233, 172–182. doi:10.1016/j.enggeo.2017.12.013

Yang, J., and Wei, L. M. (2012). Collapse of Loose Sand with the Addition of Fines: the Role of Particle Shape. *Géotechnique* 62 (12), 1111–1125. doi:10.1680/geot.11.p.062

Yao, T., Thompson, L., Yang, W., Yu, W., Gao, Y., Guo, X., et al. (2012). Different Glacier Status with Atmospheric Circulations in Tibetan Plateau and Surroundings. *Nat. Clim Change* 2 (09), 663–667. doi:10.1038/nclimate1580

Zhang, L., Ma, W., Yang, C., and Yuan, C. (20142014). Investigation of the Pore Water Pressures of Coarse-Grained sandy Soil during Open-System Step-Freezing and Thawing Tests. *Eng. Geology.* 181, 233–248. doi:10.1016/j.enggeo.2014.07.020

Zhou, G. G. D., Chen, L.-L., Mu, Q.-Y., Cui, K. F. E., and Song, D.-r. (2019). Effects of Water Content on the Shear Behavior and Critical State of Glacial till in Tianmo Gully of Tibet, China. *J. Mt. Sci.* 16 (8), 1743–1759. doi:10.1007/s11629-019-5440-9

Zimmermann, M., and Haeberli, W. (1992). Climatic change and debris flow activity in highmountain areas. *Catena supplement* 22 (1), 59–72. doi:10.1016/j.atherosclerosis.2015.04.310